# On the characterization of single-event related brain activity from functional Magnetic Resonance Imaging (fMRI) measurements*

Nafiseh Khoram[1], Chadia Zayane[2], Taous-Meriem Laleg-Kirati[2], and Rabia Djellouli[1]

*Abstract*— **We propose an efficient numerical technique for calibrating the mathematical model that describes the single-event related brain response when fMRI measurements are given. This method employs a regularized Newton technique in conjunction with a Kalman filtering procedure. We have applied this method to estimate the biophysiological parameters of the Balloon model that describes the hemodynamic brain responses. Illustrative results obtained with both synthetic and real fMRI measurements are presented.**

## I. INTRODUCTION

We consider the problem of calibrating the model that describes single-event related brain response when fMRI measurements are given. More specifically, we propose to estimate the biophysiological parameters of the so-called Balloon model, which is a dynamical system that describes the hemodynamic brain responses [1]. This problem can be formulated as an inverse problem that falls in the category of parameter identification of a dynamical system. We propose a regularized Newton method equipped with a Kalman filtering procedure to estimate these parameters from the knowledge of some fMRI measurements. The Newton component of the proposed algorithm addresses the nonlinear aspect of the problem. The regularization feature is used to ensure the stability of the algorithm. The Kalman filter is a de-noising procedure incorporated to address the noise in the data. We have conducted a numerical investigation using synthetic data tainted with various noise levels to assess the performance of the proposed method [2]. We present results to illustrate the potential of the proposed solution methodology to accurately and efficiently estimate the biophysiological parameters. These results clearly indicate that the proposed method outperforms the Cubature Kalman Filter (CKF), a procedure that is considered to be among the most successful parameter estimation techniques [3]. Finally, we also present results obtained from using real fMRI measurements corresponding to a finger-tapping stimulus.

*This work was supported by the Interdisciplinary Research Institute for the Sciences (IRIS).

[1]N. Khoram and R. Djellouli are with Department of Mathematics & IRIS, California State University Northridge (CSUN), Northridge, USA `nafiseh.khoram.25@my.csun.edu`, `rabia.djellouli@csun.edu`

[2]T. M. Laleg-Kirati and C. Zayane are with the Department of Applied Mathematics and Computational Science, King Abdullah University of Science and Technology (KAUST), KSA `taousmeriem.laleg@kaust.edu.sa`, `chadia.zayane@kaust.edu.sa`

## II. PROBLEM STATEMENT

### A. The Hemodynamic System: The Direct Problem

The problem of describing the single-event related hemodynamic brain response to an exogenous input can be formulated in the framework of the dynamical system theory. The model we consider is called the hemodynamical system (HDS) [4] which is a first-order nonlinear differential system given by:

$$(HDS) \quad \left\{ \begin{array}{ll} \dot{\vec{x}}(t) = & A(\vec{\theta};\vec{x}(t)) + \nu_t \\ \widetilde{y}(t) = & H(\vec{\theta};\vec{x}(t)) + \omega_t \quad ; \qquad\qquad t \geq 0 \\ \vec{x}(0) = & \widetilde{\vec{x}}_0 \end{array} \right. \tag{1}$$

where the component of the state vector $\vec{x}(t) = (f(t), s(t), v(t), q(t))^T$ are defined in Table I and the biophysiological system parameters $\vec{\theta} = (\alpha, \epsilon, \mathcal{K}, \mathcal{X}, \tau, E_0, V_0)^T$ are listed in Table II. The nonlinear vector-valued function$A$ describes the underlying physiology of the continuous hemodynamic system and is given by:

$$A(\vec{\theta};\vec{x}(t)) = \left\{ \begin{array}{l} s(t) \\ \epsilon u(t) - \mathcal{K}s(t) - \mathcal{X}(f(t)-1) \\ \tau(f(t) - v(t)^{1/\alpha}) \\ \tau(f(t)\frac{1-(1-E_0)^{1/f(t)}}{E_0} - q(t)v(t)^{(1/\alpha-1)}) \end{array} \right. \tag{2}$$

where $t \rightarrow u(t)$ is the prescribed control input [2], [3]. The real-valued function $H$ models the observations, that is, the Blood Oxygenation Level Dependent (BOLD) signal. $H$ is given by:

$$H(\vec{\theta};\vec{x}(t)) = V_0\left[k_1(1-q(t)) + k_2(1-q(t)/v(t)) + k_3(1-v(t))\right] \tag{3}$$

Note that $\nu_t$ (resp. $\omega_t$) is a random vector with zero mean and $4 \times 4$ positive semidefinite covariance matrix, $Q_t$ (resp. real-valued covariance, $R_t$), depending on the time $t$. $\nu_t$ (resp. $\omega_t$) represents the level and distribution of the noise in the process equations (resp. in the measurements). Hence, $\widetilde{y}(t)$ represents the noisy bold signal at time $t$. $k_1, k_2$ and $k_3$ are positive constants given by $k_1 = 7E_0$, $k_2 = 2$ and $k_3 = 2E_0 - .2$ [3].

### B. The Discrete Inverse Problem

The determination of the parameters $\vec{\theta}$ of HDS(1) from the knowledge of some BOLD signal measurements $\vec{y}$ can be formulated as the following inverse parameter problem:

978-1-4244-7929-0/14/$26.00 ©2014 European Union 

TABLE I

DESCRIPTION OF STATE VARIABLES

| State variables | Description | Values at rest |
|---|---|---|
| $f(t)$ | Cerebral blood flow | 1 |
| $s(t)$ | Flow inducing signal | 0 |
| $v(t)$ | Normalized cerebral blood volume | 1 |
| $q(t)$ | Normalized total deoxyhemoglobin content level | 1 |

TABLE II

DESCRIPTION OF THE BIOPHYSIOLOGICAL PARAMETERS

| Descriptions | Parameters |
|---|---|
| Stiffness exponent | $\alpha$ |
| Neural efficacy | $\epsilon$ |
| Rate of signal decaying | $\mathcal{K}$ |
| Rate of flow-dependent elimination | $\mathcal{X}$ |
| Hemodynamic transit time | $\tau$ |
| Resting net oxygen extraction fraction | $E_0$ |
| Resting blood volume | $V_0$ |

$$
\text{(IPP)} \quad \left\{ \begin{array}{l} \textit{Given an initial state } \widetilde{\vec{x}}_0, \textit{ a control input} \\ u(t_j) = (u(t_0), u(t_1), \ldots, u(t_M))^T, \\ \textit{and a BOLD signal } \widetilde{\vec{y}} = (\widetilde{y}_0, \widetilde{y}_1, \ldots, \widetilde{y}_M)^T, \\ \textit{find } \vec{\theta} \textit{ and } \vec{x}(t) \textit{ such that:} \\ \widetilde{H}(\vec{\theta}; \vec{x}(t_j)) = \widetilde{y}_j; \qquad j = 0, 1, \ldots, M \end{array} \right.
$$

where the tilde notation indicates a noisy quantity, $\widetilde{y}_j$ is the noisy measured BOLD signal at time $t_j$, and $M$ is the number of measurements.

## III. Parameter Estimation: The Solution Methodology

The parameter identification problem IPP is an inverse problem that is difficult to solve, especially from a numerical point of view, because it is nonlinear and ill-posed. In practice, this means that small errors in the measured BOLD signal can induce large errors in the estimate of the parameters. The proposed solution methodology is based on the Tikhonov-regularized Newton method (TNM) [5], since regularized iterative methods appear to be the primary candidates for solving nonlinear and ill-posed problems (see, e.g., [6], and the references therein). The Newton algorithm addresses the nonlinear aspect of IPP, whereas the Tikhonov regularization procedure is incorporated to address its ill-posed nature [7]. In addition, a Kalman-type de-noising procedure is built within the proposed method to filter the noise contaminating the considered model. More specifically, we employ the so-called cubature Kalman filter (CKF)[3]. To the best of our knowledge, this is the first time TNM is employed in conjunction with CKF resulting in a novel procedure with a great potential for solving IPP efficiently and accurately, as illustrated by the results reported in Section IV-A and Section IV-B. For more details about the performance and limitations of the existing numerical methods for solving IPP, the reader can see [2] and the references therein.

### A. The Regularized Newton Algorithm

The solution of the IPP by the regularized Newton algorithm incurs at each iteration m the solution of the linearized problem of the form:

$$
\begin{aligned}
&\sum_{j=1}^{M} \sum_{l=1}^{7} \frac{\partial \widetilde{H}^{(m)}}{\partial \theta_k} (\theta_l^{(m)}; \vec{x}^{(m)}(t_j)) \frac{\partial \widetilde{H}^{(m)}}{\partial \theta_l} (\vec{\theta}^{(m)}; \vec{x}^{(m)}(t_j)) \delta \theta_l^{(m)} \\
&+ \gamma \delta \theta_k^{(m)} = \sum_{j=1}^{M} \frac{\partial \widetilde{H}^{(m)}}{\partial \theta_k} (\vec{\theta}^{(m)}; \vec{x}^{(m)}(t_j)) \left( \widetilde{y}_j - y^{(m)}(t_j) \right) \\
&\qquad ; k = 1, \ldots, 7
\end{aligned} \tag{4}
$$

and then we update $\vec{\theta}^{(m+1)} = \vec{\theta}^{(m)} + \vec{\delta\theta}^{(m)}$. Note that $y^{(m)}(t) = \widetilde{H}^{(m)}(\vec{\theta}^{(m)}; \vec{x}^{(m)}(t))$, and the positive real number $\gamma$ is the Tikhonov regularization parameter. The choice of $\gamma$ is a balancing act between stability and accuracy [2]. The critical step in the numerical implementation of the regularized Newton method is the computation, at each iteration $m$, of the Jacobian $J_H^{(m)} = \left[ \frac{\partial \widetilde{H}}{\partial \theta_l} (\vec{\theta}^{(m)}; \vec{x}^{(m)}(t_j)) \right]$ for $j = 1, \ldots, M$ and $l = 1, \ldots, 7$. Such computation must be executed with a high level of accuracy to ensure the stability, fast convergence and computational efficiency of the proposed Newton algorithm. The evaluation of these derivatives requires the computation of the derivatives of the state vector $\vec{x}$ with respect to the parameters $\vec{\theta}$. We have demonstrated a theorem that shows that these derivatives are the solutions of ordinary differential systems similar to HDS(1) but with different right-hand-sides (see Theorem 1 page 20 in [2]). Note the $7 \times 7$ linear system given by Eq. (4) is inverted using a standard direct method (LU factorization).

### B. Cubature Kalman filtering

The CKF procedure is a nonlinear filtering procedure that is derivative-free and more importantly the number of integration points, called the cubature points, increases linearly with the state-vector dimension. The CKF algorithm evaluates the BOLD signal in two steps: (a) a time update step in which *predicted* estimates of the state-vector and error covariance matrix are delivered at the next time step, and (b) a measurement update step in which *corrected* estimates of the *predicted* values are calculated.

$i$-The Prediction Step in CKF. For $l = 0, 1, \ldots, M$, let $\vec{x}_l$ (resp. $P_l$) be an estimated value of the state vector $\vec{x}$ (resp. the error covariance matrix $P$) at time $t_l$. Suppose that $\vec{x}_l$ and $P_l$ have been evaluated up to $l = j$ where $j < M - 1$. Then, in order to compute $\vec{x}_{j+1}$ and $P_{j+1}$, we first calculate in this step $\widehat{\vec{x}}_{j+1}$ (resp. $\widehat{P}_{j+1}$) a *predicted* estimate of the state vector (resp. the corresponding error covariance matrix). We evaluate $\widehat{\vec{x}}_{j+1}$, by first calculating the cubature vectors as follows:

$$
\vec{c}_{i,j} = S_j \vec{\xi}_i + \vec{x}_j; \qquad i = 1, 2, \cdots, 8 \tag{5}
$$

where $S_j$ results from the Cholesky factorization of the error covariance matrix $P_j$, that is, $P_j = S_j S_j^T$ and $\vec{\xi}_i$ is the given $i^{th}$ column vector of the cubature points matrix (see Eq. 7, page 2112 in [3]). Then, using the process equation in HDS(1) and the cubature vectors calculated in Eq. (5), we solve the following first order differential system

$$
\left\{ \begin{array}{l} \dot{\vec{z}}_i = A(\vec{\theta}; \vec{z}_i) \\ \vec{z}_i = \vec{c}_{i,j} \end{array} \right. ; \qquad i = 1, \ldots, 8 \tag{6}
$$

and then evaluate the $i^{th}$ "*propagated*" cubature vectors at time $t_{j+1}$, that is, $\vec{z}_{i,j+1} = \vec{z}_i(t_{j+1})$. Note that, the differential system given by Eq. (6) is typically solved using Runge-Kutta methods of order 4.

The *predicted* estimate for the state at time $t_{j+1}$ is then calculated as follows:

$$\widehat{\vec{x}}_{j+1} = \frac{1}{8}\sum_{i=1}^{8} \vec{z}_{i,j+1} \tag{7}$$

Furthermore, the *predicted* estimate for the error covariance matrix $\widehat{P}_{j+1}$ at time $t_{j+1}$ is evaluated as follows:

$$\widehat{P}_{j+1} = \frac{1}{8}\sum_{i=1}^{8} \vec{z}_{i,j+1}\vec{\mathbf{c}}^T_{i,j+1} - \widehat{\vec{x}}_{j+1}\widehat{\vec{x}}^T_{j+1} + Q_{j+1} \tag{8}$$

where $Q_{j+1} = Q_{t_{j+1}}$ is the process noise covariance matrix defined in Section II-A.

*ii*-The Correction Step in CKF. This step is called the correction step. The goal here is to calculate $x_{j+1}$ and $P_{j+1}$ by "correcting" the predicted values $\widehat{x}_{j+1}$ and $\widehat{P}_{j+1}$, and $y_{j+1}$, the estimated BOLD signal at time $t_{j+1}$ is then deduced. To this end, we first evaluate $\vec{x}_{j+1}$ as follows:

$$\vec{x}_{j+1} = \widehat{\vec{x}}_{j+1} + (\widetilde{y}_{j+1} - \widehat{y}_{j+1})\overrightarrow{W}_{j+1} \tag{9}$$

where $\widetilde{y}_{j+1}$ is the given measured BOLD signal at time $t_{j+1}$, $\widehat{y}_{j+1}$ is the *predicted* BOLD signal at time $t_{j+1}$. It is calculated by applying the cubature quadrature rule to the measurement equation given in HDS(1) as follows:

$$\widehat{y}_{j+1} = \frac{1}{8}\sum_{i=1}^{8} H(\vec{\theta}; \widehat{\vec{c}}_{i,j+1}) \tag{10}$$

with $\widehat{\vec{c}}_{i,j+1}$ being the $i^{th}$ "*predicted*" cubature vector obtained as follows:

$$\widehat{\vec{c}}_{i,j+1} = \widehat{S}_{j+1}\vec{\xi}_i + \widehat{\vec{x}}_{j+1}; \qquad i = 1, 2, \cdots, 8 \tag{11}$$

where the matrix $\widehat{S}_{j+1}$ results from the Cholesky factorization of the *predicted* error covariance matrix $\widehat{P}_{j+1}$ at time $t_{j+1}$, that is, $\widehat{P}_{j+1} = \widehat{S}_{j+1}\widehat{S}^T_{j+1}$. $\overrightarrow{W}_{j+1}$ is the so-called *Kalman gain* at time $t_{j+1}$, and is given by:

$$\overrightarrow{W}_{j+1} = M^{-1}_{j+1}\overrightarrow{N}_{j+1} \tag{12}$$

The real number $M_{j+1}$, called the *innovation covariance* value, is given by:

$$M_{j+1} = \frac{1}{8}\sum_{i=1}^{8}\Big(H(\vec{\theta}; \widehat{\vec{c}}_{i,j+1})\Big)^2 - \widehat{y}^2_{j+1} + R_{j+1} \tag{13}$$

and $R_{j+1} = R(t_{j+1})$ is the measurement noise covariance value. The vector $\overrightarrow{N}_{j+1}$, called the *cross covariance* vector, is given by:

$$\overrightarrow{N}_{j+1} = \frac{1}{8}\sum_{i=1}^{8} H(\vec{\theta}; \widehat{\vec{c}}_{i,j+1})\vec{z}_{i,j+1} - \widehat{y}_{j+1}\widehat{\vec{x}}_{j+1} \tag{14}$$

The *corrected* error covariance matrix is then evaluated as follows:

$$P_{j+1} = \widehat{P}_{j+1} - M_{j+1}\overrightarrow{W}_{j+1}\vec{W}^T_{j+1} \tag{15}$$

where $\widehat{P}_{j+1}$, $M_{j+1}$ and $\overrightarrow{W}_{j+1}$ are given by Eqs. (8),(13) and (12) respectively.

Last, we deduce the estimated BOLD signal at time $t_{j+1}$ as follows:

$$y_{j+1} = H(\vec{\theta}, \vec{x}_{j+1}) \tag{16}$$

## IV. Illustrative Numerical Results

### A. Parameter Estimation with Synthetic Data

Because of space limitations, we present the result of one numerical experiment to illustrate the potential of the proposed solution methodology for calibrating efficiently the hemodynamical system HDS(1). In this experiment an *on-off* control input is employed, that is, $u(t)$ is a step function [2], [3].

The synthetic BOLD signal (see Figure 1) is generated by solving the noise free hemodynamical system HDS(1) with the initial state vector $\vec{x}_0 = (1, 0, 1, 1)^T$ and the biophysiological system parameters $\vec{\theta}^*$ are listed in Table III. Moreover, we consider a set of 25 measurements ($M = 25$) taken every three second ($\Delta t = 3\,\mathrm{s}$), that is, $\widetilde{\vec{y}} \in \mathbb{R}^{25}$ and $y_j = y(j\Delta t)$. The goal of this experiment is to illustrate the robustness of the method to the noise level in the measured BOLD signal. We artificially add white noise to the data as follows: 5% to $\vec{x}_0$, 1% to the process equation, and 10% to $\vec{y}$. We use a blind guess for the initial biophysiological parameters vector $\vec{\theta}^{(0)}$ whose components are all set to .5 (see Table III). The obtained results are depicted in Figures 2-3. These results were obtained with $\gamma = 18$, selected via a trial and error strategy. Note that it is possible to use other values of $\gamma$ in an interval containing 18 and obtain comparable results, as indicated in [2]. The following observations are noteworthy:

- As reported in Table III the initial parameters' values $\vec{\theta}^{(0)}$ is selected outside the pre-asymptotic convergence region. Indeed, Figure 1 shows that the use of this initial guess with HDS(1) leads to an initial BOLD signal profile that is very far from the target (the $L^2$- relative error is over 78%)
- The result depicted in Figure 2 reveals that the TNM-CKF algorithm delivers a signal with an excellent accuracy level (the relative error drops to 4.6%) which is remarkable considering the relatively high noise level in the data. Note that the relative error, in the euclidean norm, on the parameters that was initially 49% decreases monotonically and reaches 15% at convergence.
- Figure 3 indicates that TNM-CKF algorithm requires only 3 iterations to converge (the relative residual is about 8%). This performance illustrates the efficiency of the method and its robustness to the noise effect.

TABLE III

Biophysiological parameters: Target vs. initial values.

| Parameters ($\vec{\theta}$) | $\alpha$ | $\epsilon$ | $\mathcal{K}$ | $\mathcal{X}$ | $\tau$ | $E_0$ | $V_0$ |
|---|---|---|---|---|---|---|---|
| Target ($\vec{\theta}^*$) | .45 | .6 | .4 | .15 | .4 | .3 | 1.05 |
| Initial guess ($\vec{\theta}^{(0)}$) | .5 | .5 | .5 | .5 | .5 | .5 | .5 |

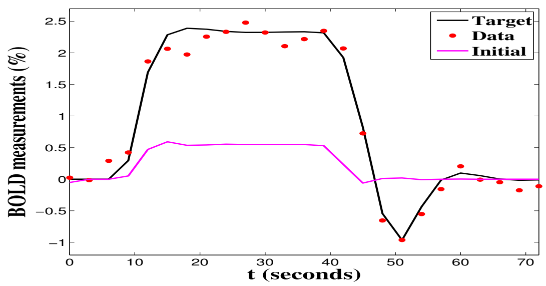


Fig. 1. Synthetic BOLD signal profiles: Target (solid-black). Measured with 10% white noise (dotted-red) and Initial (solid-magenta).

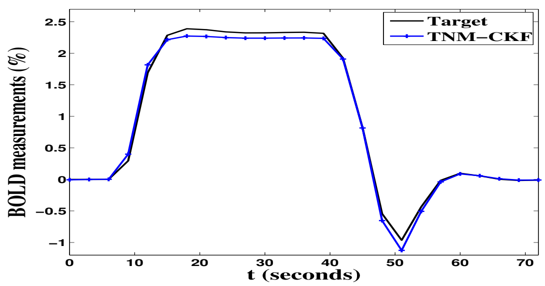


Fig. 2. Synthetic BOLD signal profiles: Target (black). Computed with TNM-CKF (blue).

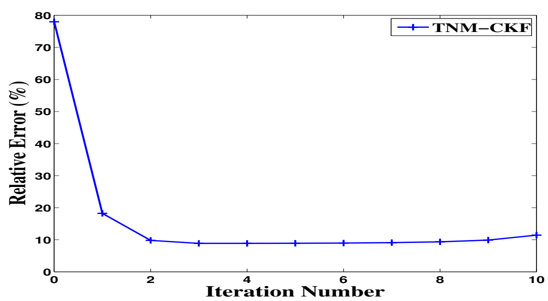


Fig. 3. Convergence history of the TNM-CKF algorithm in the case of synthetic measurements.

### B. Parameter Estimation with Real Data

We consider here the case of real fMRI measurements corresponding to a face-repetition stimulus [8]. More specifically, famous and non-famous faces were presented twice against a check board baseline. The subject was asked to make fame judgement by making key presses [8]. We applied the TNM-CKF using 385 BOLD measurements, $\vec{\theta}^{(0)}$ given in Table III, $\vec{x}_0 = (1, 0, 1, 1)^T$, and an *on-off* control input. Figure 4 indicates that TNM-CKF delivers a BOLD signal with an excellent accuracy level (about 12% relative error) and Figure 5 demonstrates the convergence of the TNM-CKF algorithm after only 15 iterations.

## V. CONCLUSIONS

The TNM-CKF algorithm is a solution methodology that is conceptually simple to understand and implement. The calibration results obtained with both synthetic and fMRI

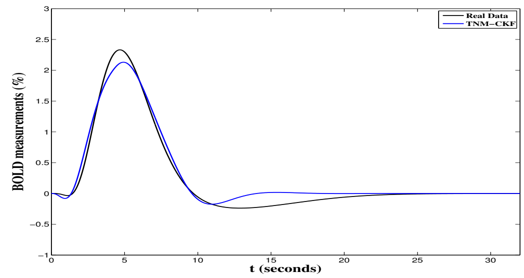


Fig. 4. BOLD signal profiles: Real (black) vs. Computed (blue).

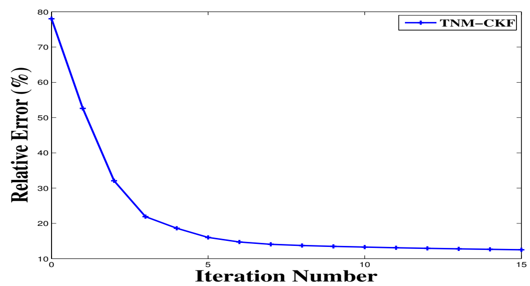


Fig. 5. Convergence history of the TNM-CKF algorithm in the case of real measurements.

measurements clearly indicate that TNM-CKF algorithm is robust to the noise effect and requires few iterations to converge to an accurate solution even when starting with an initial guess value of the parameters outside the pre-assymptotic convergence region.

## ACKNOWLEDGMENT


The authors would like to thank Dr. Nasser Kashou, Wright State University for the enlightening discussions.


## REFERENCES


[1] K. J. Friston, E. Zarahn, O. Josephs, R. Henson, and A. Dale, "Stochastic design in event-related fMRI," *NeuroImage*, vol. 10, pp. 607–619, 1999.

[2] N. Khoram, "On the characterization of single-event related brain activity from functional magnetic resonance imaging (fmri) measurements," Master's thesis, California State University, Northridge, 2013. [Online]. Available: `http://www.csun.edu/~iris/2012-2013.htm`

[3] M. Havlicek, K. J. Friston, J. Jan, M. Brazdil, and V. D. Calhoun, "Dynamic modeling of neuronal responses in fmri using cubature kalman filtering," *Neuroimage.*, vol. 56, no. 4, pp. 2109–28, Jun 2011.

[4] K. J. Friston, "Variational filtering." *NeuroImage*, vol. 41, no. 3, pp. 747–66, Jul. 2008.

[5] S. F. Gilyazov and N. L. Goldman, *Regularization of ill-posed problems by iteration methods*. Kluwer Academic Publishers, 2000.

[6] R. Djellouli, *Inverse Acoustic Problems, in: Computational Methods for Acoustic Problems*. Saxe-Coburg Publications, 2008.

[7] V. Y. Tikhonov, A. N.; Arsenin, *Solutions of Ill-Posed Problems*. New York: Winston, 1977.

[8] T. F. M. Group, *SPM8 Manual*, February 2013. [Online]. Available: `http://www.fil.ion.ucl.ac.uk/spm/doc/manual.pdf`